

***In vivo* optical coherence tomography detection of differences in regional large airway smoke inhalation induced injury in a rabbit model**

Matthew Brenner

University of California, Irvine
Beckman Laser Institute
Irvine, California 92612
and

University of California, Irvine Medical Center
Pulmonary and Critical Care Division
Orange, California 92868
E-mail: mbrenner@uci.edu

Kelly Kreuter

University of California, Irvine
Beckman Laser Institute
Irvine, California 92612

Johnny Ju

University of California, Irvine Medical Center
Pulmonary and Critical Care Division
Orange, California 92868

Sari Mahon

University of California, Irvine
Beckman Laser Institute
Irvine, California 92612

Lillian Tseng

University of California, Irvine Medical Center
Pulmonary and Critical Care Division
Orange, California 92868

David Mukai

Tanya Burney
Shuguang Guo
Jianping Su

University of California, Irvine
Beckman Laser Institute
Irvine, California 92612

Andrew Tran

University of California, Irvine Medical Center
Pulmonary and Critical Care Division
Orange, California 92868

Andriy Batchinsky

Leopoldo C. Cancio

United States Army Institute of Surgical Research
Fort Sam Houston, Texas

Navneet Narula

University of California, Irvine Medical Center
Pathology Division
Orange, California 92868

Zhongping Chen

University of California, Irvine
Beckman Laser Institute
Irvine, California 92612

Abstract. Smoke inhalation injury causes acute airway injury that may result in airway compromise with significant morbidity and mortality. We investigate the ability of high resolution endobronchial optical coherence tomography (OCT) to obtain real-time images for quantitatively assessing regional differences between upper tracheal versus lower tracheal and bronchial airway injury responses to smoke inhalation *in vivo* using a prototype spectral domain (SLD)-OCT system we constructed, and flexible fiber optic probes. 33 New Zealand White rabbits are intubated and mechanically ventilated. The treatment groups are exposed to inhaled smoke. The OCT probe is introduced through the endotracheal tube and maintained in place for 5 to 6 h. Images of airway mucosa and submucosa are obtained at baseline and at specified intervals postexposure. Starting within less than 15 min after smoke inhalation, there is significant airway thickening in the smoke-exposed animals. This is maintained over 5 h of imaging studies. The lower tracheal airway changes, correlating closely with carboxyhemoglobin levels, are much greater than upper tracheal changes. Significant differences are seen in lower trachea and bronchi after acute smoke inhalation compared to upper trachea as measured *in vivo* by minimally invasive OCT. OCT is capable of quantitatively detecting regional changes in airway swelling following inhalation injury. © 2008 Society of Photo-Optical Instrumentation Engineers. [DOI: 10.1117/1.2939400]

Keywords: optical coherence tomography; smoke inhalation injury; bronchial; tracheal; fiber optic probe.

Paper 07349R received Aug. 25, 2007; revised manuscript received Dec. 17, 2007; accepted for publication Dec. 22, 2007; published online Jun. 23, 2008.

1 Introduction

Smoke inhalation injury is a major cause of morbidity and mortality among victims of fires. Pathophysiologic changes include hyperemia, edema, sloughing, and necrosis, which can cause airway compromise and acute lung injury.¹⁻⁹ Currently, there are no highly reliable diagnostic techniques in the clinical setting to predict or assess the degree of airway com-

Address all correspondence to Matthew Brenner, Pulmonary and Critical Care Division, Univ. of California/Irvine, 101 City Dr South, Building 53, Rm 119 Orange, CA 92868; Tel: 714 456 5150; Fax: 714 456 8349; E-mail: mbrenner@uci.edu

promise following smoke inhalation. High-resolution flexible fiber optic optical coherence tomography (OCT) provides the potential to observe real-time changes in the airway mucosa and epithelium using minimally invasive imaging techniques.¹⁰⁻²⁵ Most importantly, some of the early pathologic changes following smoke inhalation that may be indicative of the extent of injury such as edema and hyperemia^{2,26-29} may not be apparent clinically, endoscopically, or following histologic preparations of excised specimens, but can be readily detected on OCT.³⁰

Previous OCT airway injury studies³⁰ in rabbit smoke inhalation models suggested to us that the upper trachea airway may react very differently to acute smoke inhalation compared to distal trachea and proximal bronchi. The purpose of this study was to demonstrate the potential role of OCT in quantitatively detecting early smoke inhalation injury and assessing differences in response of more proximal versus distal large airways to smoke inhalation injury.

2 Materials and Methods

This protocol was approved by the University of California, Irvine (UCI) Academic Research Committee (2002-2397) and complied with all federal and state regulations for animal welfare assurance. General model and preparation methods have been described previously³⁰ and are briefly summarized here.

2.1 General Preparation

33 male New Zealand White rabbits, weighing 3 to 5 kg (Western Oregon Rabbit Company, Philomath, Oregon) were anesthetized with a 2:1 ratio of ketamine HCl (100 mg/ml) (Ketaject, Phoenix Pharmaceutical Incorporated, Saint Joseph, Michigan): xylazine (20 mg/ml) (Anased, Lloyd Laboratories, Shenandoa, Iowa), 0.75-cc/kg IM using a 23 gauge 5/8 in. needle. After the IM injection, a 23 gauge 1-in. catheter was placed in the marginal ear vein to administer IV maintenance anesthetic of a 1:1:3 mixture of ketamine:xylazine:saline (Ketamine 100 mg/ml: xylazine 20 mg/ml) as a continuous infusion, at a rate of 0.17 ml/min. A dose of analgesic, Torbutrol 0.1 to 0.5 mg/kg SQ, was administered prior to intubation. The animals were orally intubated with a 3.5-mm cuffed endotracheal tube and mechanically ventilated (dual phase control respirator, model 613, Harvard Apparatus, Chicago, Illinois) at a respiratory rate of 32/min and a tidal volume of 60 cc and FiO₂ of 100%. A humidifier (Humid-Vent mini Ref. 10011, Hudson RCI, Temecula, California) was positioned between the ventilator and endotracheal tube to prevent drying out of the mucosa, which could result in airway changes due to prolonged exposure to ventilated O₂. On completion of the experiment, the animals were euthanized with an intravenous injection of Eutha-6 (1.0-2.0 cc) administered through the marginal ear vein.³⁰

2.2 Systemic Arterial Blood Pressure, Blood Gas Analysis, and Co-Oximetry

Femoral arterial and venous cutdowns were performed to collect blood samples and record systemic blood pressure. An 18 gauge catheter (C-PMA-400-FA, Cook Incorporated, Bloomington, Indiana) was inserted into the vein and artery, and a three-way stop-cock was placed on the ends. To measure systemic arterial pressure, a calibrated pressure trans-

ducer (TSD104A Transducer and MP100 WSW System, Biopac Systems, Incorporated, Santa Barbara, California) was connected to a pulmonary artery extension set, which was then attached to the end of the stop-cock. Blood was drawn from both the arterial and venous lines and measured by a blood gas analyzer (IRMA SL Series 2000 Blood Analysis System, Diametrics Medical Incorporated, Saint Paul, Minnesota) to obtain arterial and venous blood gas analysis, respectively. On-site co-oximetry measurements (AVOXimeter 4000, AVOX Systems, San Antonio, Texas) were conducted to measure oxyhemoglobin, carboxyhemoglobin, methemoglobin fractions, and total hemoglobin. The carboxy Hgb levels were analyzed to assess the degree of smoke exposure. The co-oximeter was calibrated with rabbit blood by the manufacturer for the research purposes in these studies.

2.3 Administration of Smoke

Smoke was administered according to the previously published protocol.³⁰ 70 g of unbleached cotton was burned in a modified bee smoker (Smoke Stack Smoker 644, Brushy Mountain Bee Farm, Moravian Falls, North California) for approximately 20 min. The bee smoker was then connected to the inlet port of the mechanical ventilator with the tidal volume and ventilation rate set at 700 ml and 25 breaths per minute, respectively. A Mylar Douglas bag (model 6060, Hans Rudolph, Kansas City, Missouri) was connected to a second "smoke exposure" ventilator (ventilator 2) (also a dual phase control respirator, model 613, Harvard Apparatus, Chicago, Illinois) via the multiport valve to the output port to actively fill the bag with smoke from the bee smoker, and over 25 L of smoke was collected. The Mylar bag was then connected to the inlet port of the smoke exposure ventilator and set to a tidal volume of 60 ml and a ventilation rate of 18 breaths per minute to deliver the (now cool) smoke-filled contents of the Douglas bag to the rabbit in a controlled manner. The rabbit was disconnected from the regular ventilator (1) circuit and connected to the smoke ventilator (2) for exposure. Exposure was achieved by giving the animal repetitive alternate increments of 18 breaths of smoke, followed by 100% oxygen (accomplished by switching between the traditional ventilator setup and the smoke ventilator). For smoke exposure, rabbits were ventilated with 0 breaths of smoke (controls) or a variable number of breaths of smoke (smoke group). The range of smoke breaths administered was between 54 and 216 breaths (mean 127 breaths) that were administered by alternating a minimum of three cycles of 18 breaths of cooled smoke with nine breaths of ventilated O₂ (*i.e.*, a minimum of 54 breaths in the treatment groups). Co-oximetry measurements were taken at the end of smoke exposure. To obtain a broad range of carbon monoxide levels, additional breaths were given to some animals to raise the carboxyhemoglobin levels throughout the desired dosage range. Carboxyhemoglobin measurements of between 0.2 and 48% were obtained in the exposure group animals.

2.4 Optical Coherence Tomography System and Probes

The OCT system used in this study contains a superluminescent diode source that delivers an output power of 10 mW at

a central wavelength of 1310 nm with a full width at half maximum (FWHM) of 80 nm, resulting in approximately 10- μ m axial resolution.³⁰

In the reference arm, a rapid-scanning optical delay line is used that employs a grating to control the phase and group delays separately, so that no phase modulation is generated when the group delay is scanned. The phase modulation is generated through an electro-optic phase modulator that produces a carrier frequency. The axial line scanning rate is 500 Hz, and the modulation frequency of the phase modulator is 500 kHz. Reflected beams from the two arms are recombined in the interferometer and detected on a photodetector. The detected optical interference fringe intensity signals are bandpass filtered at the carrier frequency. Resultant signals are then digitized with an analog-digital converter, which performs 12 bit at 5-MHz signal conversion and is transferred to a computer where the structural image is generated.^{12,19,31}

Flexible fiber optic OCT probes were constructed from a single mode fiber (ThorLabs, Newton, New Jersey). The bare-ended fiber was attached to a 0.7-mm-diam gradient index (GRIN) lens (NSG America, Irvine, California), using optical adhesive (Dymax Company, Torrington, Connecticut) under a microscope. A right angle-light path was achieved using a 0.7-mm prism. The probe was placed in fluorinated ethylene propylene tubing (17 gauge thin wall, Zeus, Orangeburg, South Carolina) for added fiber support. The outer diameter of the probe is approximately 2 mm.

A linear motor (Newport Instruments, Irvine, California) was used to drive the coated flexible fiber optic distally and proximally along the length of the probe within the sheath, moving the GRIN lens and prism imaging components within the sheath to obtain linear images along the long axis of the trachea and bronchi. Axial scans were obtained every 10 μ m along the length of the probe during 16-mm-long scan sweeps. A 16-mm scan is obtained in 3.2 sec. Translational imaging has a number of distinct theoretical advantages over rotational scanning methods for initial investigations in relatively large lumen sites such as trachea and proximal bronchi. These advantages include that the translational probe can be placed in the trachea at any location, as long as it is not touching the tissue itself; whereas the rotational probe would have to be centered in the trachea, the translational probe can be fixed in a location, and doing this with a rotational probe would be difficult (a fraction of a movement with the rotational probe would yield false results); and finally, the translational probe can only capture a fraction of the image.^{12,19,31}

2.5 Airway Thickness Measurements

Airway thickness was measured as the distance between the epithelial surface and the surface of landmark submucosal cartilaginous rings in the trachea and bronchi, and includes epithelial, subepithelial, and glandular tissues above the cartilage.³⁰ Measurements were obtained by two independent researchers (Ju and Tseng) who were blinded to all clinical information. Airway thickness measurements were taken at as many landmark cartilaginous rings as could be seen in an individual animal (generally 3 to 5 cartilage ring sites per animal). Measurements of the airway thickness at the landmark rings were obtained at baseline, and at each specified time period following inhalation injury. Approximately nine

measurements were taken per time point. The percent change from baseline was calculated for each airway thickness measurement at every time point. Values were then averaged for all airway thickness measurements within a given animal at each specified point.

2.6 Upper Trachea Versus Lower Trachea/Bronchi Placement

Upper trachea was defined in this study to be within 5 cm below the larynx, and lower trachea/bronchi to be below that level. For lower trachea/bronchi studies, the standard 3.5-mm endotracheal tube (16 cm length) was advanced fully down the trachea and secured in position. The OCT probe was then placed through the endotracheal tube just beyond the tip of the tube. For upper tracheal measurements, the 3.5-mm-diam endotracheal tube was cut to a length of 14 cm prior to insertion, advanced to approximately 2 cm from maximal insertion distance, and secured in place. With this approach, the tip of the endotracheal tube usually resided in the upper trachea. Due to variability in positioning and tracheal length, the actual position of the OCT probe, and therefore the animal group, was definitively determined with certainty only at the time of sacrifice.

2.7 Statistical Analysis

Differences between controls, and upper and lower trachea/bronchi were determined by analysis of variance. A two-tailed p value less than 0.05 was considered statistically significant. For descriptive statistics, mean \pm standard error is reported. Correlations were assessed using standard linear regression. All statistical analysis was performed using commercial statistical software (Systat 10, SPSS, Incorporated, 2002).

3 Results

30 animals total were exposed to inhaled room-temperature smoke for this study (mean 127 ± 9 breaths, range from 54 to 216 breaths total). 14 animals were in the lower trachea/bronchi exposure group, 16 in the upper tracheal exposure group, and 3 controls (no smoke exposure). As seen in our previous studies, the smoke-treated animal study groups had significant increases in airway thickness seen by *in vivo* OCT. Changes were evident in the thickness of the airway mucosa at the time of the first follow-up measurement 15 min following exposure with an average increase in airway thickness of $27 \pm 5\%$ (SEM) for the overall smoke-treated animals ($p < 0.001$).²¹ No change was seen in the airway thickness of the control group animals (three upper and ten lower airway) that were not exposed to smoke during the first 60 min of anesthesia, intubation, and ventilator support administered in an analogous manner to the smoke-treatment animals. A slight increase in the mucosal thickness of the control group was observed during the experiments, although this increase was not significant. This increase was most likely due to the positive pressure of the ventilator or the anesthesia, as these are both known to cause effects similar to the ones we observed. Despite the marked changes in the subepithelial layers seen on OCT, only epithelial cell layer changes were seen on histologic examination (Fig. 1).

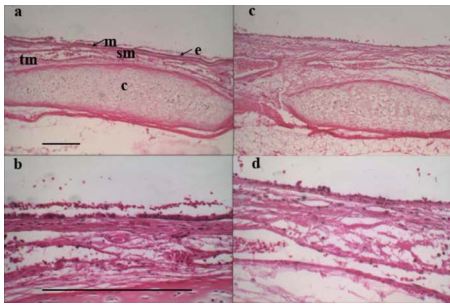


Fig. 1 (a) Histology showing upper rabbit trachea taken (10× objective) 6-h postsmoke exposure (the notable landmarks are: c-cartilage ring, e-epithelium, m-mucosa, sm-submucosa, and tm-muscularis). (b) Histology of upper rabbit trachea shown 6-h postsmoke exposure (40× objective). (c) Lower rabbit trachea 6-h postsmoke exposure (10× objective). (d) Lower rabbit trachea 6-h postsmoke (40× objective). Reference bars represent 0.25 mm.

Carboxyhemoglobin levels were obtained immediately postexposure in 26 of the 33 animals studied (7 lower trachea, 19 upper trachea). The range of carboxyhemoglobin levels

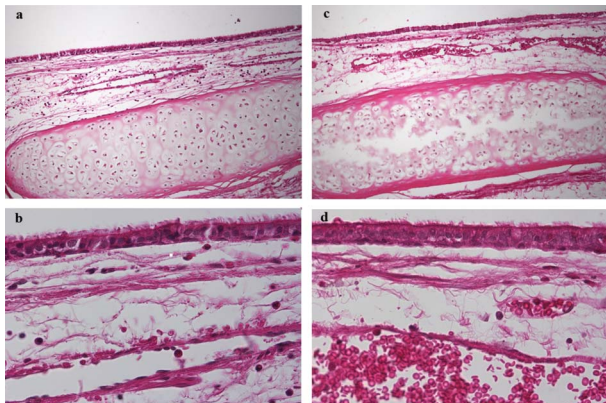


Fig. 2 (a) Histology image of normal rabbit lower trachea (10× objective). (b) Normal rabbit lower trachea (40× objective). (c) Normal rabbit upper trachea (10× objective). (d) Normal rabbit upper trachea (40× objective).

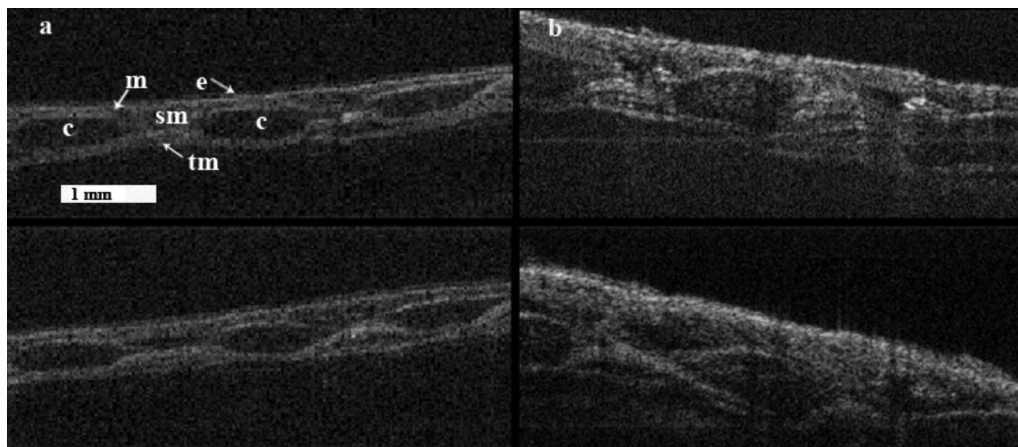


Fig. 3 (a) Longitudinal *in vivo* OCT image showing baseline upper trachea (top) and the same upper trachea 360 min following smoke exposure (bottom) (the notable landmarks are: c-cartilage rings, e-epithelium, m-mucosa, sm-submucosa, and tm-muscularis). (b) Longitudinal OCT image showing baseline low trachea (top) and the same trachea 360 min after smoke exposure (bottom). Reference bar represents 1 mm.

attained in the smoke-treated animals was $21.7 \pm 2.7\%$ overall (range 0.2 to 46.7%), while the control group averaged $1.0 \pm 0.4\%$ percent (range 0.2 to 1.7%), ($p < 0.02$). There was no significant difference in the average carboxyhemoglobin levels in the upper trachea group (mean $22.7 \pm 2.9\%$, range 8.6 to 42.5%) versus lower trachea/bronchi (mean $19.8 \pm 2.9\%$, range 0.2 to 46.7%) ($p = 0.68$). There was no difference in the total number of smoke breaths administered to the upper tracheal group (mean 141 ± 11 breaths, range 90 to 198) versus the lower trachea/bronchi (mean 110 ± 13 breaths, range 54 to 216) ($p = ns$).

Regional differences were seen in the degree of airway thickness changes following smoke exposure in the lower trachea/bronchi in comparison to the upper tracheal exposure groups when the OCT images at baseline were compared to those images taken 360 min after smoke exposure (Fig. 2). Statistically significant increases from baseline were seen in the lower trachea/bronchi treated animal group at all time periods postexposure (Fig. 3). At 15-min postexposure, the lower trachea/bronchi treated group showed a $29 \pm 7\%$ increase in airway thickness compared to baseline ($p < 0.001$). Airway thickness peaked in at 240 to 300-min postexposure with a mean increase of $85 \pm 22\%$ increase ($p < 0.003$). The upper trachea smoke-exposed animals also showed early increases in mucosal thickness at 15-min postexposure ($25 \pm 8\%$ increase, $p < .007$). However, no significant further increases occurred after 15 to 30 min (at 30 min $r = 0.36$, $r^2 = 0.13$, $p = 0.23$, and at 240 min $r = 0.14$, $r^2 = 0.02$, and $p = 0.66$), with airway swelling peaking at 30-min postexposure at a $29 \pm 7\%$ increase from baseline ($p < 0.001$). The degree of airway swelling from baseline was statistically significantly higher in the lower trachea/bronchi groups compared to the upper tracheal group beginning at 180-min postexposure; $21 \pm 7\%$ for the upper group versus $76 \pm 14\%$ increase for the lower trachea/bronchi ($p < 0.002$) (Fig. 4). These differences continue to increase out to 300-min postexposure ($25 \pm 8\%$ increase for the upper group versus $85 \pm 22\%$ increase for the lower trachea/bronchi group, $p < 0.02$ at 300 min).

Smoke Induced Changes in Airway Thickness

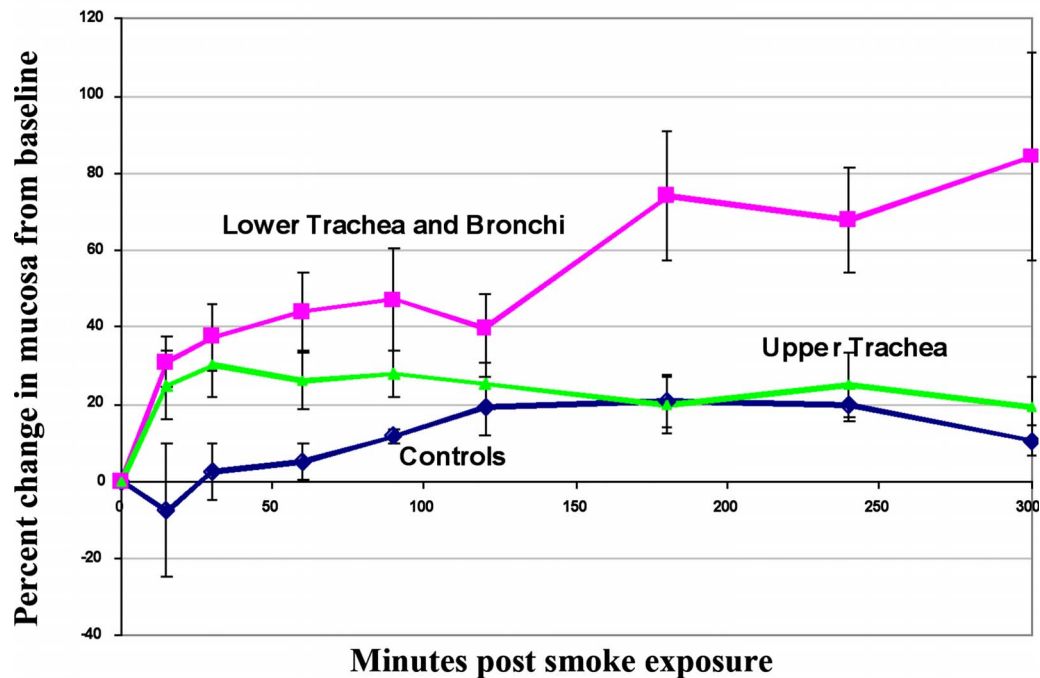


Fig. 4 Percent change in airway thickness of trachea and bronchi from baseline following smoke exposure or controls over time as measured by *in vivo* OCT. Control animals showed a gradual, mild increase in airway thickness that became statistically significant after two hours, but leveled off at that time. Upper tracheal regions showed early increases in airway thickness that were statistically significant within 15 min following exposure, peaked at 30 min, and remained stable out to five hours postexposure. In contrast, lower trachea and proximal bronchi showed early and progressive increases in airway thickness over time to 4 to 5 h. The difference increase in airway thickness changes following smoke exposure between lower trachea and bronchi groups versus upper tracheal injury groups was statistically significant.

To further explain the individual animal and regional variability in airway response to smoke exposure, the degree of airway thickness changes was correlated with carboxyhemoglobin levels attained for the upper trachea group in comparison to the lower trachea/bronchi group. In the lower trachea/bronchi group, there was a very close correlation between the degree of airway thickening and the carboxyhemoglobin level beginning at the first follow-up measurement period, 15-min postexposure ($r=0.83$, $r^2=0.70$, $p<0.01$, $n=7$), and this trend continued to be observed at 30-min postexposure ($r=0.86$, $r^2=0.74$, $p=0.01$, $n=7$), and 240-min postexposure ($r=0.75$, $r^2=0.56$, $p=0.05$, $n=7$) (Fig. 5). This close correlation was maintained throughout the postexposure measurement period as the airway swelling progressed. In contrast, in the upper trachea group, no correlation was seen at any time period postexposure between the degree of upper tracheal swelling and carboxyhemoglobin levels.

4 Discussion

This study demonstrated the ability of optical coherence tomography minimally invasive imaging to detect acute changes in airway thickening following inhalation smoke exposure at various levels within the trachea and proximal bronchi. Optical coherence tomography images used in this study were obtained in real time at resolutions of $10\ \mu\text{m}$ using flexible fiber optic GRIN lens-based probes and were capable of providing a mean to quantitatively assess the degree of airway

thickness through measurements of the images. The changes could be monitored continuously, as in this study, for more than five hours following smoke exposure. Previous studies using this model³⁰ have shown that substantial airway changes occur very early after room temperature smoke exposure. The current study was designed to use OCT to assess regional response differences in the degree of airway changes seen in the upper trachea compared to lower trachea/bronchi following smoke exposure. The ability to quantitatively measure such differences with OCT is important for understanding potential regional variability mechanisms in inhalation injury *in vivo*, and will be important in future studies designed to correlate acute injury with subsequent pathophysiologic events.

This study demonstrated substantial statistically and clinically significant differences in the degree of airway changes occurring in the upper trachea compared to proximal bronchi and distal trachea. Variable but dramatic increases were seen in the thickness of the lower trachea/bronchial airways, while only modest changes developed in the higher trachea. These changes began very early following smoke exposure, frequently being observed within five minutes following exposure.

We are uncertain why the upper trachea and lower large airway regions may have responded so differently. There may be inherent differences in sensitivity to smoke in upper trachea versus distal trachea and bronchi. It is possible that the differences result from differences in deposition of smoke par-

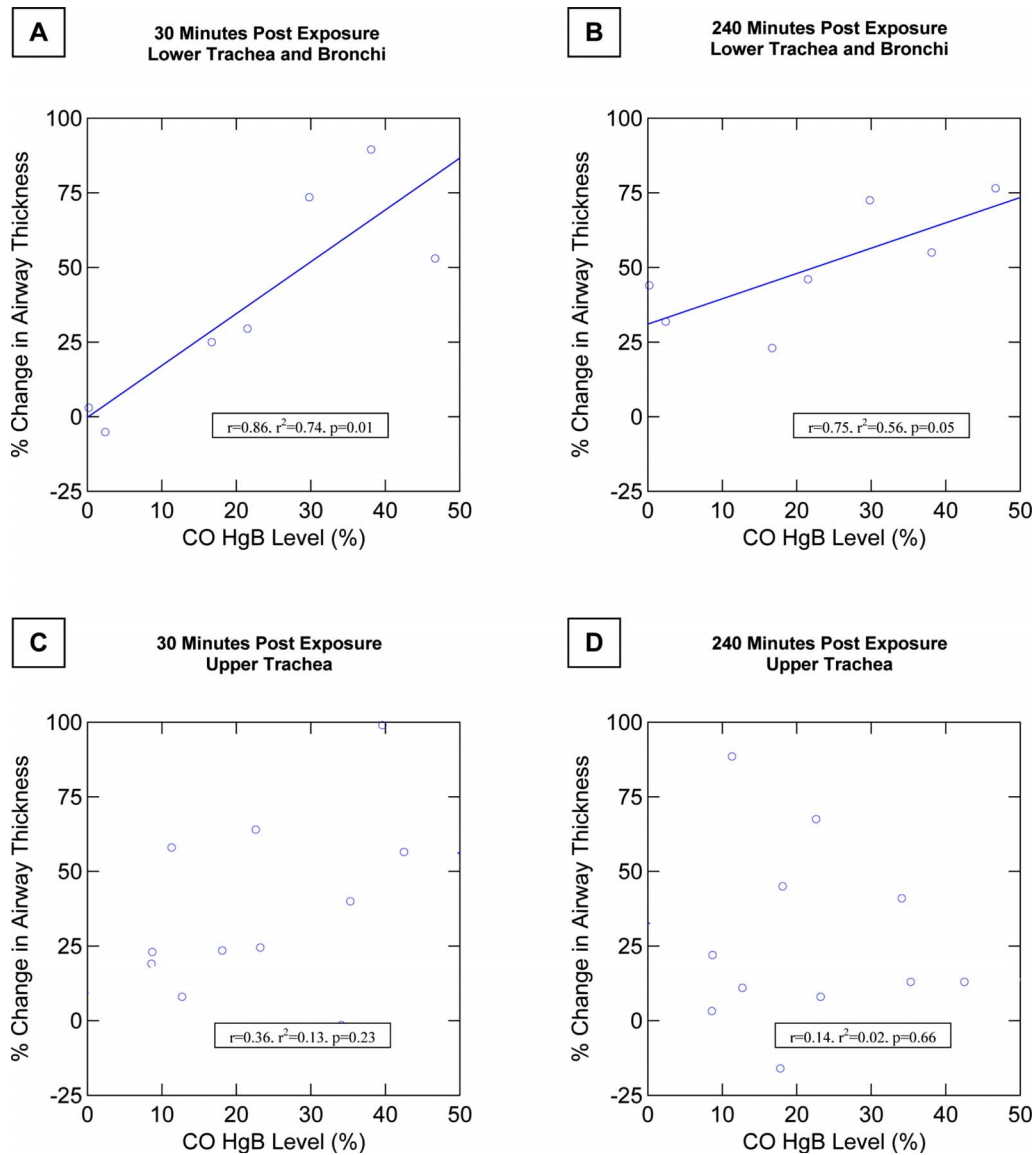


Fig. 5 Increases in airway thickness following smoke exposure correlated closely with the exposure dose as measured by arterial carboxyhemoglobin levels in animals in the lower trachea and proximal bronchi injury group. This close correlation was seen early as well as later following smoke exposure. (a) Graph shows the correlation between percent change in airway thickness and carboxyhemoglobin level at 30-min postexposure in the lower trachea and bronchi injury group. (b) Graph shows the correlation in this group at 240 min (four hours) postexposure. (c) Graph shows absence of relationship between airway thickness and carboxyhemoglobin levels in the upper trachea exposed animals at 30-min postexposure. (d) Graph shows similar lack of correlation at 240-min postexposure.

ticles in the distal trachea and bronchi following smoke exposure. The smoke exposure was performed with room-temperature smoke administered down the endotracheal tube of intubated animals. For the upper tracheal assessments, the endotracheal tube was cut short (14 cm length). For the lower trachea/bronchi assessments, the endotracheal tube was kept at full length. Thus, the tip of the endotracheal tube (where the smoke exits and exposure can begin) was equidistant from the OCT probe in both cases. It is possible that the diameter and curvature of the lower trachea and bronchi result in toxic particle impaction with resultant increase in airway injury. Prior studies have shown that tracheobronchial injury in smoke inhalation is primarily due to toxic chemicals contained in the smoke.² Future studies will be needed to further clarify the causes for these regional differences, and may be very impor-

tant to understanding the nature of inhalation injury and improving treatment/outcomes.

There are a number of limitations with these studies. It was not until the time of sacrifice that the position of the endotracheal tube and optical coherence tomography probe was determined with certainty. It was not possible to precisely place the OCT probe in the right main stem bronchus at specific locations prior to smoke treatment with this study design. Furthermore, the imaging direction of the OCT probe was generally pointed anteriorly (as evidenced by as the presence of cartilaginous rings and continuous airway wall). However, the exact angle of imaging was not clearly defined, and precise delineation of distal trachea from proximal bronchi, or right versus left mainstem bronchi, could not be determined until after sacrifice.

The exact pathophysiology of the airway injury seen on OCT is also uncertain. The very early appearance of the changes suggests that edema and/or hyperemia may be predominant components of the injury process. The findings are consistently present on OCT evaluation. However, a proportion of the airway thickening changes seen on OCT disappears immediately following sacrifice, six hours postexposure. This would suggest that previously described hyperemia^{1,2,26,27} in the initial stages following smoke exposure may be a significant component of this process. Furthermore, histology of the tracheal specimens following sacrifice does not demonstrate significant changes from controls, even in animals that had dramatic changes seen on OCT; this is consistent with published literature and suggests edema or hyperemia as major components of the early injury process that are lost during histologic preparation.

Imaging with small diameter flexible fiber optic white-light bronchoscopy showed only mild evidence of early hyperemia following smoke exposure. Regional deposition of smoke particles could not be differentiated visibly, and as expected, the degree of airway swelling could not be determined by fiber optic bronchoscopy, despite significant changes seen on OCT.

Thermal effects are unlikely a significant component of these findings, because room-temperature smoke was used and thermal injury would be expected to be more severe closer to the tip of the endotracheal tube.²

Carboxyhemoglobin levels were obtained in the animals as a marker of the degree of exposure. A range of carbon monoxide levels was obtained in animals through variation in numbers of administered smoke-containing breaths, as well as intrinsic variability in the level of carboxyhemoglobin achieved for a given number of breaths. The average carboxyhemoglobin levels achieved and the total number of smoke breaths administered were not statistically significantly different between the upper trachea and distal trachea exposure groups, and were actually slightly higher in the upper trachea group where less effect was seen. Therefore, greater degrees of airway swelling in the lower trachea/bronchial injury group could not be explained by greater degrees of total smoke exposure.

Interestingly, the degree of airway swelling correlated very closely with the level of carboxyhemoglobin attained in the animals during the postexposure period in the lower trachea/bronchi group. This is evidence of a dose-response relationship between total smoke exposure and early airway injury effects in this lower tracheal and proximal bronchial region.³² In contrast, more upper trachea showed significantly less injury, and no correlation with carboxyhemoglobin levels at any time following exposure.

Future studies to further elucidate the causes behind the regional differences in response to smoke injury, association between airway changes and various pathologic mediators of tissue injury and repair, as well as correlation between early changes and later effects are needed.

Flexible fiber optic optical coherence tomography is minimally invasive, and can be performed with very narrow diameter flexible probes that can be left in place to image intermittently or continuously. This can potentially facilitate follow up evaluations of smoke inhalation injury, which progresses over time,^{1,2,26,27,33} and that may not be evident during bronchoscopic evaluation. This study was able to demonstrate that

OCT has the capability of not only detecting changes in thickness in the layers of the mucosa, but also quantifying differences in the magnitude of changes in the upper and lower trachea. The ability of OCT to distinguish such changes in real time may someday assist clinically in determining the extent of injury, prognosis, and need for intervention. Quantitative determination of acute and longer term changes in the airway epithelium, mucosa, and submucosa with OCT may also provide a more sensitive tool for investigation of the effectiveness of various therapeutic interventions in smoke inhalation and other airway injuries.

Acknowledgments

This work was supported by Department of Defense: AFOS-2004-0011A and 0012A, AF-9550-04-1-0101, LAMMP 445474-30136, NIH CA-91717, and EB-000293.

References

1. R. A. Cox, A. S. Burke, K. Soejima, K. Murakami, J. Katahira, L. D. Traber, D. N. Herndon, F. C. Schmalstieg, D. L. Traber, and H. K. Hawkins, "Airway obstruction in sheep with burn and smoke inhalation injuries," *Am. J. Respir. Cell Mol. Biol.* **29**(3 Pt 1), 295–302 (2003).
2. D. L. Traber, H. A. Linares, D. N. Herndon, and T. Prien, "The pathophysiology of inhalation injury—a review," *Burns Incl Therm Inj* **14**(5), 357–364 (1988).
3. R. L. Cecil, L. Goldman, and J. C. Bennett, *Cecil Textbook of Medicine*, W. B. Saunders, Philadelphia (2000).
4. D. R. Thorming, M. L. Howard, L. D. Hudson, and R. L. Schumacher, "Pulmonary responses to smoke inhalation: morphologic changes in rabbits exposed to pine wood smoke," *Hum. Pathol.* **13**(4), 355–364 (1982).
5. R. L. Sheridan, "Airway management and respiratory care of the burn patient," *Int. Anesthesiol. Clin.* **38**(3), 129–145 (2000).
6. T. Muehlberger, D. Kunar, A. Munster, and M. Couch, "Efficacy of fiber optic laryngoscopy in the diagnosis of inhalation injuries," *Arch. Otolaryngol. Head Neck Surg.* **124**(9), 1003–1007 (1998).
7. M. J. Masanes, C. Legendre, N. Lioret, R. Saizy, and B. Lebeau, "Using bronchoscopy and biopsy to diagnose early inhalation injury. Macroscopic and histologic findings," *Chest* **107**(5), 1365–1369 (1995).
8. M. J. Masanes, C. Legendre, N. Lioret, D. Maillard, R. Saizy, and B. Lebeau, "Fiber optic bronchoscopy for the early diagnosis of subglottal inhalation injury: comparative value in the assessment of prognosis," *J. Trauma* **36**(1), 59–67 (1994).
9. T. L. Palmieri, "Inhalation injury: research progress and needs," *J. Burn Care Res.* **28**(4), 549–554 (2007).
10. Y. Yang, S. Whiteman, D. G. van Pittius, Y. He, R. K. Wang, and M. A. Spiteri, "Use of optical coherence tomography in delineating airways microstructure: comparison of OCT images to histopathological sections," *Phys. Med. Biol.* **49**(7), 1247–1255 (2004).
11. M. Brenner, H. Poggemeyer, W. Jung, M. Krutzik, J. Lee, P. Tran, and Z. Chen, "High resolution non-invasive optical coherence tomography imaging of airways," *Chest* **122** S(4), 31S (2002).
12. S. Han, N. H. El-Abbadi, N. Hanna, U. Mahmood, R. Mina-Araghi, W. G. Jung, Z. Chen, H. Colt, and M. Brenner, "Evaluation of tracheal imaging by optical coherence tomography," *Respiration* **72**(5), 537–541 (2005).
13. T. Xie, S. Guo, Z. Che, D. Mukai, and M. Brenner, "GRIN lens rod based probe for endoscopic spectral domain optical coherence tomography with fast dynamic focus tracking," *Opt. Express* **14**(8), 3238–3245 (2006).
14. U. Mahmood, N. M. Hanna, S. Han, W. G. Jung, Z. Chen, B. Jordan, A. Yershov, R. Walton, and M. Brenner, "Evaluation of rabbit tracheal inflammation using optical coherence tomography," *Chest* **130**(3), 863–868 (2006).
15. J. G. Fujimoto, W. Drexler, U. Morgner, F. Kartner, and E. Ippen, "Optical coherence tomography: high resolution imaging using echoes of light," *Opt. Photonics News* **11**(1), 24–31 (2000).
16. J. G. Fujimoto, B. E. Bouma, G. J. Tearney, S. A. Boppart, C. Pitris, J. Herrmann, E. A. Swanson, J. F. Southern, and M. E. Brezinski,

- "Optical coherence tomography for biomedical imaging and diagnostics," *12th International Conference on Optical Fiber Sensors. Technical Digest*, pp. 2–6 (1997).
17. G. J. Tearney, B. E. Bouma, S. A. Boppart, M. E. Brezinski, J. F. Southern, E. A. Swanson, and J. G. Fujimoto, "Endoscopic optical coherence tomography," *Proceedings of the Institute of Electrical and Electronics Engineers, Lasers and Electro-Optics Society, Annual Meeting*, pp. 328–329, Vol. **321** (1996).
 18. G. Sutedja, "New techniques for early detection of lung cancer," *Eur. Respir. J. Suppl.* **39**, 57s–66s (2003).
 19. J. Woonggyu, Z. Jun, P. B. B. Wilder-Smith, M. Reza, M. Brenner, S. YongJin, J. S. Nelson, and C. Zhongping, "Optical coherence tomography in pulmonary imaging: feasibility study," *Proc. SPIE* **5316**, 44–55 (2004).
 20. S. C. Whiteman, Y. Yang, D. Gey van Pittius, M. Stephens, J. Parmer, and M. A. Spiteri, "Optical coherence tomography: real-time imaging of bronchial airways microstructure and detection of inflammatory/neoplastic morphologic changes," *Clin. Cancer Res.* **12**(3 Pt 1), 813–818 (2006).
 21. M. Brenner, K. Kreuter, D. Mukai, T. Burney, S. Guo, J. Su, S. Mahon, A. Tran, L. Tseng, J. Ju, and Z. Chen, "Detection of acute smoke-induced airway injury in a New Zealand white rabbit model using optical coherence tomography," *J. Biomed. Opt.* **12**(5), 051701 (2007).
 22. G. J. Tearney, I. K. Jang, and B. E. Bouma, "Optical coherence tomography for imaging the vulnerable plaque," *J. Biomed. Opt.* **11**(2), 021002 (2006).
 23. Y. Chen, A. D. Aguirre, P. L. Hsiung, S. Desai, P. R. Herz, M. Pedrosa, Q. Huang, M. Figueiredo, S. W. Huang, A. Koski, J. M. Schmitt, J. G. Fujimoto, and H. Mashimo, "Ultrahigh resolution optical coherence tomography of Barrett's esophagus: preliminary descriptive clinical study correlating images with histology," *Endoscopy* **39**(7), 599–605 (2007).
 24. L. P. Hariri, A. R. Tumlinson, D. G. Besselsen, U. Utzinger, E. W. Gerner, and J. K. Barton, "Endoscopic optical coherence tomography and laser-induced fluorescence spectroscopy in a murine colon cancer model," *Lasers Surg. Med.* **38**(4), 305–313 (2006).
 25. X. D. Li, S. A. Boppart, J. Van Dam, H. Mashimo, M. Mutinga, W. Drexler, M. Klein, C. Pitris, M. L. Krinsky, M. E. Brezinski, and J. G. Fujimoto, "Optical coherence tomography: advanced technology for the endoscopic imaging of Barrett's esophagus," *Endoscopy* **32**(12), 921–930 (2000).
 26. D. N. Herndon, R. E. Barrow, H. A. Linares, R. L. Rutan, T. Prien, L. D. Traber, and D. L. Traber, "Inhalation injury in burned patients: effects and treatment," *Burns Incl Therm Inj* **14**(5), 349–356 (1988).
 27. K. Murakami and D. L. Traber, "Pathophysiological basis of smoke inhalation injury," *News Physiol. Sci.* **18**, 125–129 (2003).
 28. A. Bidani, H. K. Hawkins, C. Z. Wang, and T. A. Heming, "Dose dependence and time course of smoke inhalation injury in a rabbit model," *Lung* **177**(2), 111–122 (1999).
 29. L. C. Cancio, A. I. Batchinsky, M. A. Dubick, M. S. Park, I. H. Black, R. Gomez, J. A. Faulkner, T. J. Pfannenstiel, and S. E. Wolf, "Inhalation injury: pathophysiology and clinical care proceedings of a symposium conducted at the Trauma Institute of San Antonio, San Antonio, TX, USA on 28 March 2006," *Burns* **33**, 681–692 (2007).
 30. M. Brenner, K. Kreuter, D. Mukai, T. Burney, S. Guo, J. Su, S. Mahon, A. Tran, L. Tseng, J. Ju, and Z. Chen, "Detection of acute smoke induced airway injury in a new zealand white rabbit model using optical coherence tomography," *J. Biomed. Opt.* **12**, 051701 (2007).
 31. N. Hanna, D. Saltzman, D. Mukai, Z. Chen, S. Sasse, J. Milliken, S. Guo, W. Jung, H. Colt, and M. Brenner, "Two-dimensional and 3-dimensional optical coherence tomographic imaging of the airway, lung, and pleura," *J. Thorac. Cardiovasc. Surg.* **129**(3), 615–622 (2005).
 32. M. S. Park, L. C. Cancio, A. I. Batchinsky, M. J. McCarthy, B. S. Jordan, W. W. Brinkley, M. A. Dubick, and C. W. Goodwin, "Assessment of severity of ovine smoke inhalation injury by analysis of computed tomographic scans," *J. Trauma* **55**(3), 417–427; discussion 427–419 (2003).
 33. H. M. Loick, L. D. Traber, J. C. Stothert, D. N. Herndon, and D. L. Traber, "Smoke inhalation causes a delayed increase in airway blood flow to primarily uninjured lung areas," *Intensive Care Med.* **21**(4), 326–333 (1995).